Age structure and recharge conditions of a coastal aquifer (northern Germany) investigated with ^{39}Ar, ^{14}C, ^{3}H, He isotopes and Ne

Jürgen Sültenfuß · Roland Purtschert · Jens F. Führböter

Abstract A tide-influenced two-layer aquifer system in northern Germany was investigated using environmental dating tracers (^{3}H, ^{39}Ar, ^{14}C), the noble gas isotopes ^{3}He, ^{4}He and Ne. The study area is a marshland at the River Ems estuary, exposed to regular flooding until AD 1000. The construction of dykes, artificial land drainage and groundwater abstraction define the hydraulic gradient. The aquifer depicts a pronounced age stratification with depth. Tritium concentrations above 0.03 TU are found only in the top 30 m. Two tritium-free samples between 20 and 30 m depth show ^{39}Ar ages of 130 and 250 years. Below a clay layer–about 50 m below surface level (mbsl)–all analysed samples are ^{39}Ar free and, thus, older than 900 years. The initial ^{14}C activities were about 70 pmC. Resulting ^{14}C ages increase with depth and increase up to 9,000 years, in agreement with minimal ^{39}Ar ages. Concentrations of radiogenic ^{4}He correlate with ^{14}C ages. Samples in a mid-depth range (20–70 mbsl) show significant gas loss. The gas loss is assigned to recharge in a methane producing environment. Deduced ^{4}He ages were used to assign this water to a infiltration period of about AD 1000.

Received: 1 February 2010 / Accepted: 1 October 2010
Published online: 30 October 2010

J. Sültenfuß (✉)
Institute of Environmental Physics,
University of Bremen,
Otto-Hahn-Allee, 28359, Bremen, Germany
e-mail: suelten@uni-bremen.de

R. Purtschert
Climate and Environmental Physics,
University of Bern,
Sidlerstrasse 5, 3012, Bern, Switzerland

J. F. Führböter
Leichtweiß Institute for Hydraulic Engineering
and Water Resources,
Technical University of Braunschweig,
Beethovenstr. 51a, 38106, Braunschweig, Germany

Keywords Coastal aquifers · Groundwater age · Radioactive isotopes · Tracers · Germany

Introduction

About 65% of the world population lives close to a coastline, within less than 150 km. This number could increase up to 75% by 2025 (Hinrichsen 1998) and water supply could become a serious problem. Coastal aquifers are complex salt–freshwater systems, featuring hydraulic interaction with local aquifers. For the future use of coastal aquifers for local water supply, it is essential to understand such systems under present and past hydraulic conditions. In most cases, an anthropogenic impact on natural hydraulic conditions, like for example intensive water withdrawal in coastal areas, will not have an immediate influence on the salinity of the extracted drinking water. However, in the long-term, these aquifers could be lost for water supply for decades if saline water reaches the production wells. Especially for old groundwater resources, which recharged under different climatic conditions than today, a change of hydraulic conditions could lead to serious quality problems.

A number of Dutch scientists have published work about saltwater-intrusion problems, especially on the Dutch coast (Stuyfzand 1996), which is similar to the situation in northern Germany. The River Ems estuary aquifer system in northwest Germany is threatened by the intrusion of brackish water from the tidal-influenced River Ems. Close to the river, production wells of the water supplier Stadtwerke Emden GmbH extract high quality groundwater mainly from a Pliocene aquifer. The mosaic of fresh- and saltwater-dominated aquifer sections within the two-aquifer system could not be explained only by the heterogeneous geological structures and the present-day hydraulic system. It is more likely that time-variable groundwater flow regimes and mixing are the reasons for the present-day salt-freshwater distribution (Führböter 2004). This dating study should contribute to knowledge of the regional-scale groundwater dynamics.

With the set of environmental tracers consisting of ^{3}H, ^{39}Ar, ^{14}C, He isotopes and Ne the groundwater age was

 DOI 10.1007/s10040-010-0663-4

studied on a larger scale in proximity to the production wells. The applied tracer set covers a dating range of years to millennia and allows for investigation of the hydraulic conditions with respect to human activity during the last hundreds of years.

Hydrogeology of the Ems estuary aquifer system

The study area is located at the Ems estuary near the city of Emden (Fig. 1). Following the cross-section in Fig. 1 from A to B (shown in the final Fig. 12), the area is divided into the tidal influenced River Ems, the marshlands, relict Geest cores within the marshland, peat bogs at the edges of the Upper Geest, and the Upper Geest in the east. The term *Geest* is used for the typical landscape in northern Germany, The Netherlands and Denmark, and is formed by glacial sediments of the Pleistocene. The Oldenburg-Ostfriesischer Geest ridge is morphologically characterized by the NW–SE striking structure with a maximum elevation of about 8 m above sea level. In particular, the glacial-fluviatile sediments of the Elster ice age formed aquifers for local water supply. With the beginning of the Holocene North Sea transgression, episodical flooding formed peat bogs at the edges of the Geest and the marshlands between the Geest and today's coastline. Within the marshland, the Pleistocene sediments are covered by a layer consisting of clay and silt with embedded sandy layers of varying thickness. The bottom of the Pliocene aquifer layer is ~140 m below sea level (mbsl). The lithology is characterized by a varying mixture of fine sand, coarse sand and gravel. The upper Pleistocene aquifer is locally separated from the lower Pliocene aquifer (sand and gravel) by a clay layer called the 'Tergast Ton' at a depth of about 50 mbsl near the village of Tergast and 30 mbsl near the village of Neermoor. The Pleistocene glacial-fluviatile sands are interbedded with layers of fine- to medium-sized sands, usually getting coarser, sometimes pebbly, towards the base of the aquifer. Local silt and clay layers with different contents of fine sands are common. The aquifers are silica-dominated sands with a variable content of feldspar and mica and low carbonate content. The average hydraulic conductivities are about 10^{-5} m/s for fine-sized sands and up to 10^{-3} m/s for gravel layers in both aquifers.

Hydraulic conditions

The natural hydraulic gradient follows the morphology of the land surface. Groundwater flows from the Upper Geest to the North Sea and River Ems. The natural groundwater surface in the marshland is at sea level. About AD 1000 the natural hydraulic conditions changed. With the construction of dykes the flooding of the marshlands stopped. The artificial drainage of the marshland decreased the piezometric head of groundwater to about 1 m below sea level. Between the River Ems and a band of about a few kilometres from the river to the mainland the natural flow direction changed direction and caused intrusion of brackish river water (Führböter 2004). Since the end of the nineteenth century, the groundwater withdrawal by production wells at the relict Geest core of Tergast (see Fig. 1) increased the hydraulic gradient from the river to the mainland (Führböter 2004).

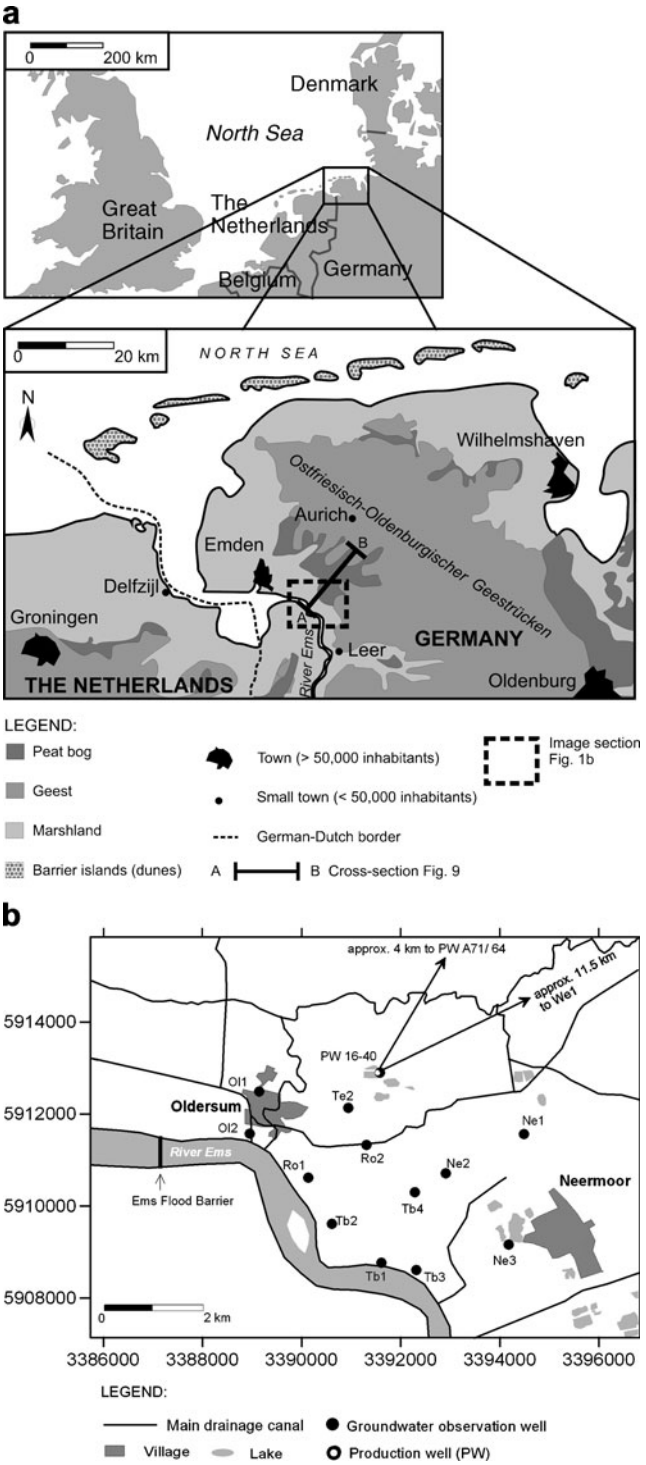

Fig. 1 **a** Study area with the major structure elements of the landscape of Ostfriesland (Eastern Frisia), northern Germany. The cross-section *A–B* marks the central part of the study area (Cartesian German National Grid: Gauß-Krüger coordinates). **b** Location of sampled observation and production wells and major surface water features

DOI 10.1007/s10040-010-0663-4

The major groundwater recharge takes place within the Upper Geest. Relict Geest cores are sources for local groundwater recharge. The groundwater recharge varies from 22–33 mm/yr in the marshland up to 200 mm/yr at the Upper Geest. In the transition zone between Upper Geest and the marshland with the peat bog areas the groundwater recharge varies within a range from 50 up to 100 mm/yr. The mean annual precipitation of 767 mm/yr is distributed equally through the year (Stadtwerke Emden 2006). Evaporation peaks from May to September and amounts to about 500 mm/yr (Hanauer B, Lenz W, Führböter JF, HG Consult/TU Braunschweig, unpublished report, 2008)

The production wells of Tergast and Simonswolde extracted about 3.5 million m^3 in 2005 mainly from the Pliocene aquifer (Stadtwerke Emden 2006). There are only estimates of the amount of interaction of shallow groundwater and the drainage canals within the marshland. During intense pumping of the drainage canals, usually during the winter, varying chloride concentrations are measured within the canal system (Schöniger M, Wolff J, Führböter JF, Jagelke J, TU Braunschweig, unpublished report, 2003). This suggests that a small amount of brackish groundwater is removed from the aquifer and mixes with the low mineralized surface water. A general correlation between the chloride concentration in shallow groundwater and varying chloride concentration in the drainage canals was not apparent. The exchange of water between the canals and shallow groundwater depends on the thickness of the cover layer and the depth and construction of the canal bed as well as on the varying hydraulic gradient between groundwater and canal.

Materials and methods

In the area of investigation, 31 observation wells are located in the marshland between the River Ems and the Geest ridge (Fig. 1). Screens are within the upper or the lower aquifer with maximum screen depths listed in Table 1. The screen length is typically 2 m, but for some observation wells length is 4 m. The observation wells are grouped in well galleries. Samples were collected during four sampling campaigns, in 2002, March 2006, July 2006 and May 2007. To cover the complex salt-freshwater distribution between River Ems and the water catchment Tergast, 29 observation wells within the rectangle Oldersum-Tergast-Neermoor-Terborg, two representative production wells (one for each catchment, labelled as PW in Fig. 1b) and two observation wells at the edge of the Upper Geest were chosen. As a reference sample, not influenced by drainage during the last 1,000 years, an observation well (Gk372) on a Geest ridge 50 km to the southeast was also sampled.

Tritium-helium dating

Radioactive tritium (^{3}H) was released in large quantities into the atmosphere between 1955 and 1963 as a result of atmospheric thermonuclear testing (e.g. Solomon and Cook 2000). The ^{3}H concentration in precipitation in the northern hemisphere displayed a maximum in 1963, with concentrations three orders of magnitude above the natural concentrations. A groundwater dating method based on the analysis of ^{3}H combined with its decay product, the lighter and rare helium-3 isotope (^{3}He), was first suggested by Tolstikhin and Kamenskiy (1969). In the saturated zone, ^{3}He produced by ^{3}H decay accumulates in the groundwater and does not undergo any chemical reactions. The derived apparent piston flow ^{3}H–^{3}He ages are therefore independent of the ^{3}H input concentration. The ^{3}H–^{3}He age of a sample refers mainly to the water components with the highest concentration. In mixtures with broad age distributions, the ^{3}H–^{3}He age is therefore biased towards the age of water which recharged during the bomb peak. The ^{3}H–^{3}He dating method has been used in many groundwater studies (e.g. Torgersen et al. 1979; Weise and Moser 1987; Schlosser et al. 1988; Solomon et al. 1993 and Szabo et al. 1996). An overview is given in Solomon and Cook (2000). Stute et al. (1997), Beyerle et al. (1999), Massmann et al. (2008) and Massmann et al. (2009) applied the method to date bank filtrate with an apparent age of several months to decades.

Tritium concentrations in water are preferentially given as hydrogen isotope ratios: 1 tritium unit (TU) equals 10^{-18} ^{3}H/^{1}H. ^{3}He produced by decay of ^{3}H, called tritiogenic ^{3}He$_{tri}$, can be converted to TU units: 1 TU equals $2.49\cdot10^{-12}$ ^{3}He$_{tri}$ cm^3 STP/kg water (STP = standard temperature and pressure). The apparent ^{3}H–^{3}He age (τ) provides a measure for the time difference between the last contact of the water with the atmosphere and the measurement and is given by:

$$\tau = \frac{1}{\lambda} \cdot \ln\left(1 + \frac{^3He_{tri}}{^3H}\right) \quad (1)$$

Where $\lambda = \ln(2)/t_{1/2}$ is the decay constant and $t_{1/2}$ is the half-life of ^{3}H (12.32 yrs; Lucas and Unterweger 2000). ^{3}He$_{tri}$ must be separated from other ^{3}He sources in the water which are:

1. ^{3}He$_{equi}$: Concentration at equilibrium conditions with the atmosphere, which is a function of temperature, salinity and atmospheric pressure during infiltration. ^{3}He$_{equi}$ is calculated with the solubility function of Weiss (1971). Isotopic fractionation was adapted according to Benson and Krause (1980).
2. ^{3}He$_{excess}$: Additional air dissolved in the water from the (partial) dissolution of air bubbles that are trapped in the quasi saturated soil zone (Aeschbach-Hertig et al. 1999). Because neon (Ne) has no sources in the aquifer the excess air component can be derived by the deviation of the Ne concentration in the sample from the calculated air-saturated equilibrium Ne concentration Ne$_{equi}$ and is called ΔNe: $\Delta Ne = \left(\frac{Ne_{sample}}{Ne_{equi}} - 1\right) \cdot 100$ in %. Negative ΔNe values indicate degassing of the water.
3. ^{3}He$_{rad}$: Produced in rocks and subsequently released to the water. ^{3}He$_{rad}$ is produced via ^{3}H by a neutron capture reaction of lithium (^{6}Li(n,α)^{3}H→^{3}He). Neu-

DOI 10.1007/s10040-010-0663-4

Table 1 Data / results of noble gas analysis and age dating

Sample ID/ screen depth (mbsl)	Sampling period (month/year)	Tritium (TU)	ΔNe (%)	$^{3}He_{trit}$ (TU)	^{3}H–^{3}He age (yrs)	$^{4}He_{rad}$ (cm^3 STP/kg) $\Delta=\pm10^{-6}$	^{14}C in TDIC/CH_4 (pmC)	^{13}C in TDIC (‰)	^{14}C age (yrs)	^{39}A (%mod)	^{39}Ar age (yrs)
Ro1/22	3/2006	0.00	–68	0	>80	2.0E-5	-/55.9				
Ro1/22	7/2006	0.00	–67	0	>80	1.8E-5				71±9	130±50
Ro1/70	3/2006	0.03	2		>80	2.10E-4					
Ro1/70	7/2006	0.05	6	4	>70	2.80E-4	51.2/-	–7.4	3,010	5±5	>900
Ro2/14	3/2006	1.00	–27	5	33[d]	1.0E-5					
Ro2/24	3/2006	1.23	–8	6.0	30[d]	1.45E-5					
Ro2/61	3/2006	0.00	–3	1	>80	1.14E-4					
Ro2/61	7/2006	0.00	–6	3	>80	1.17E-4	60.9/-	–4	1,850	5±5	>900
Tb1/18	6/2002	6.57	–20	26	29	0					
Tb1/18	5/2007	6.84	–27	45	36	0					
Tb2/12	7/2006	7.80	–12	23	24	0					
Tb2/12	5/2007	7.75	–7	22	24	0					
Tb2/12	6/2002	10.3	–1	23	21	0					
Tb2/25	7/2006	0.00	–24	0	>80	4.5E-6				52±8	250±60
Tb2/68	3/2006	-	10	0	-	1.10E-4					
Tb2/68	7/2006	-	5	2	-	1.10E-4	59.7/64.3	–8.2	1,670	5±5	>900
Tb3/15	5/2007	16.2	–11	39	21	0					
Tb3/27	2/2003	25.0	–11	36	16	0					
Tb3/27	5/2007	18.4	–11	39	20	0					
Tb3/66	3/2006	0.00	–13	3	>80	2.1E-5					
Tb4/15	6/2002	0.07	-	-	[d]	-					
Tb4/15	5/2007	0.01	–35	2	>80	2.05E-5					
Tb4/30	3/2006	0.00	–40		>80	1.05E-5					
Tb4/30	5/2007	0.00	–40	1	>80	1.57E-5					
Tb4/64	3/2006	0.00	–18	2	>80	1.0E-5					
Tb4/64	7/2006	0.00	–18	3	>80	1.0E-5	60.8/65.1	–1.9	2,040	5±5	>900
Ne1/24	3/2006	5.50	–38	42	38[d]	6E-6					
Ne1/59	3/2006	-	–42	2	-	1.1E-5	68.6/-	3.9	1,490		
Ne2/25	3/2006	0.16	–24	7	[d]	8E-6					
Ne2/62	3/2006	0.00	–29	3	>80	1.00E-4	61.6/-	1.8	2,220		
Ne3/24	3/2006	0.44	–66	3	[d]	2E-6					
Ne3/61	3/2006	0.00	–23	3	>80	6E-6					
Ol1/21	3/2006	0.03	–70	0	>80	2.1E-5					
Ol1/39	3/2006	0.00	–65	0	>80	3.0E-5					
Ol1/71	3/2006	0.00	–33	0	>80	8.0E-5					
Ol1/71	7/2006	0.00	–36	1	>80	7.6E-5	50.8/50.53	0.7	3,730		
Ol2/20	6/2002	1.42	–43	7	31[d]	4.85E-5					
Te2/5	5/2007	10.0	18	2	4	0					
Te2/12	5/2007	7.49	16	67	41	4.28E-5					
Te2/72	5/2007	0.09	–10		[d]	3.15E-4					
Te2/113	5/2007	0.06	15		[d]	6.39E-4					
We1/35[a]	3/2006	0.00	–40	0	>80	4.0E-5					
We1/35[a]	7/2006	0.00	–40	2	>80	3.9E-5					
We1/75[a]	3/2006	0.00	17	9	>80	4.90E-4					
We1/75[a]	7/2006	0.00	-		>80	-	23.7/-	–8.1	9,320	5±5	>900
PW 16-40[b]	3/2006	-	–7	8	-	4.00E-4					
PW A71/64[b]	3/2006	0.03	–12	1	>80	1.90E-4					
PW A71/64[b]	7/2006	0.05	–20	4	>70	2.04E-4	53.2/68.63	1.6	3,410	5±5	>900
Gk372/90[c]	7/2006	0.00	22	2	>80	0	63/-	–21.6	0	80±5	90±50

[a] Observation well, not on the map

[b] Production/abstraction well (screen length 15 m and 27 m)

[c] Inland reference well

[d] Water contains significant concentration of tritium. If an age is presented, this refers to the tritium-bearing portion.

Ages denoted by *>70* and *>80* are not calculated by Eq. 1. Minimum ages are derived from an estimated natural tritium concentration of 4 TU in precipitation, and hence the infiltrated water, and the calculated decay time to obtain the measured tritium concentration

- quantities not available

trons are generated by (α,n) reactions with α-particles from nuclides of the uranium (U) and thorium (Th) decay series and major matrix elements (Si, O, Al, Mg). Concentrations of radiogenic ^{3}He in water are small in general and derived from concentrations of radiogenic ^{4}He. The radiogenic $^{3}He/^{4}He$-ratio is about $2{\cdot}10^{-8}$ (Mamyrin and Tolstikhin 1984), a factor of 70 smaller than the atmospheric ratio ($R_a=1.384{\cdot}10^{-6}$).

 DOI 10.1007/s10040-010-0663-4

The tritiogenic ^{3}He is therefore given by:
$^3He_{tri} = {}^3He_{sample} - {}^3He_{equi} - {}^3He_{excess} - {}^3He_{rad}$. Long filter screens, dispersion and, in the case of production wells, convergence of flow paths will form water with a spectrum of ages rather than one age which could be specified by a single value for the ^{3}H–^{3}He age.

Radiogenic ^{4}He (^{4}He$_{rad}$) is produced by α-decay of nuclides from the U and Th decay series in the aquifer matrix. ^{4}He$_{rad}$ can be used as a qualitative age indicator (Solomon 2000) and is simply calculated as remainder: $^4He_{rad} = {}^4He_{sample} - {}^4He_{equi} - {}^4He_{excess}$. If the resulting ^{4}He$_{rad}$ accumulation rate in the water is constant in time and space within the aquifer, the ^{4}He$_{rad}$ concentration increases linearly with time and represents relative age differences. The method has been applied in old systems with apparent groundwater ages between 10^3 and 10^8 years (Andrews and Lee 1979; Torgersen and Clarke 1985). However, Solomon et al. (1996) showed that it is also possible to detect ^{4}He$_{rad}$ in young groundwater with an age of 10–10^3 years if the groundwater originates from a shallow aquifer of recently eroded sediments. In these sediments ^{4}He$_{rad}$ was accumulated in the source rock and released after erosion subsequently to the water with high rates.

Analysis

Tritium samples were collected in glass bottles. Water for noble gas analysis was pumped with a submersible pump (Grundfos MP1) through a transparent hose into a copper tube (volume 40 ml, outer diameter 1 cm). A regulator clamp was attached to the outlet of the copper tube and used to increase pressure in order to suppress potential degassing. The transparent hose was always checked for bubbles. Pumping proceeded until steady-state conditions with regard to temperature and electrical conductivity were reached. The copper tubes were subsequently pinched off with stainless steel clamps to maintain high vacuum tight sealing.

Analysis of ^{3}H, He isotopes and Ne for ^{3}H–^{3}He dating was conducted at the noble gas laboratory of the Institute of Environmental Physics, University of Bremen (Germany). For the He isotope and Ne analysis all gases were extracted from water. He and Ne were separated from other gases with a cryogenic system kept at 25 and 14 K, respectively. ^{4}He and ^{20}Ne were measured with a quadrupole mass spectrometer (Balzers QMG112A). Helium isotopes were analyzed with a high-resolution sector-field mass spectrometer (MAP 215-50). The system was calibrated with atmospheric air and controlled for stable conditions for the He and Ne concentrations and the ^{3}He/^{4}He ratio. For groundwater samples, the precision of the He and Ne concentrations is better than 1% and for the ^{3}He/^{4}He ratio better than 0.5%. ^{3}H was analysed with the ^{3}He–ingrowth method (Clarke et al. 1976). Samples of 500 g of water were degassed and stored for the accumulation of the ^{3}H decay product (^{3}He) in dedicated He-free glass bulbs. After a storage period of 2–3 months ^{3}He was analyzed with the mass spectrometric system.

For this study a detection limit of 0.03 TU was achieved which allows the detection of the residue of natural, pre-bomb ^{3}H. The uncertainty is less than 3% for samples of >1 TU and 0.03 TU for very low concentrations. For ideal samples, these analytical conditions allow a time resolution of about 6 months for apparent ages less than 10 years. Unknown hydrogeological conditions affecting gas exchange, as for example inaccurate temperatures assumed for gas exchange with the atmosphere lead to a time resolution of about 1.0 year (Kipfer et al. 2002). More details of the sampling, analysis and data evaluation of the method are given in Sültenfuss et al. (2009).

^{39}Ar dating method

^{39}Ar is produced by the interaction of cosmic rays with nuclides of potassium and argon in the atmosphere. The resulting atmospheric equilibrium activity expressed as % modern in relation to recent air (100 %modern) is unaffected by anthropogenic sources and constant at 1.67×10^{-2} Bq/m^3 of air (Loosli 1983), corresponding to an atmospheric ^{39}Ar/Ar ratio of ~10^{-15}. With a half-life of 269 years, ^{39}Ar fills the precision dating gap between the young residence time indicators (e.g. ^{3}H–^{3}He, ^{85}Kr) and the radiocarbon method.

The subsurface residence time of groundwater can be simply estimated using the radioactive decay equation and the measured decrease in ^{39}Ar compared to the initial activity in the atmosphere. A possible complication is ^{39}Ar produced in the subsurface due to neutron activation of potassium (^{39}K(n,p)^{39}Ar). If not considered in the age calculation, this would lead to an underestimation of the calculated groundwater residence time. However, elevated ^{39}Ar concentrations due to underground production rates have only been observed in rare cases within fractured rock aquifers with high U and Th concentration in the rock matrix (Andrews et al. 1989; Purtschert et al. 2007).

Sampling and analysis

Because of the very low isotopic abundance of ^{39}Ar, a relatively large amount of water (> 1,500 L) has to be degassed in the field to obtain a sufficient number of ^{39}Ar atoms. In contrast to other gaseous tracers which rely on absolute concentrations of dissolved constituents (e.g. CFC, SF_6 or ^{4}He), the ^{39}Ar method is insensitive to the degree of degassing (both in nature and during sampling) and recharge conditions because the method is based on an isotope ratio of the same element (^{39}Ar/Ar). However, for waters with depleted gas concentration, a corresponding larger sample volume is required. The ^{39}Ar activity of the argon separated from groundwater is measured in high pressure proportional counters in an ultra-low background environment (Loosli and Purtschert 2005). Although first attempts have been made to use the accelerated mass spectrometry (AMS) technique (Collon et al. 2004), which would reduce this volume, the detection of ^{39}Ar is currently only practical by the radioactive decay-counting techniques (Loosli 1983). Counting times

 DOI 10.1007/s10040-010-0663-4

range typically between 1 and 4 weeks, depending on the extracted amount of argon and the age of the water. The minimum detection level (MDL) is 3–10 %modern for water volumes of 4–1.5 tons of air-saturated water respectively.

^{14}C dating method

Radiocarbon dating of total dissolved inorganic carbon (TDIC) is one of the most widely used applications of radiocarbon dating (Kalin 2000). However, the interpretation of ^{14}C results from groundwater is complex because carbon in groundwater may be derived from several sources with different ^{14}C concentrations. Natural atmospheric ^{14}C is produced in the upper atmosphere by the reaction of thermal neutrons, which are produced by cosmic rays, with nitrogen: $^{14}N + n \rightarrow {}^{14}C + p$. The resulting equilibrium activity in the atmosphere is 100 % modern carbon (pmC) corresponding to 0.23 Bq/g_C (Kalin 2000).

^{14}C is oxidised to CO_2 and mixes into the lower atmosphere where it is assimilated in the biosphere and hydrosphere. $^{14}CO_2$ of the soil zone dissolves in the infiltrating water and ^{14}C decays in the sub-surface with a half life of 5,730 years. The radiocarbon age of the water is calculated based on the radioactive decay law:

$$A_{14C} = A_0 \cdot \exp(-\lambda_{14C} \cdot t) \quad (2)$$

where λ_{14C} is the decay constant of ^{14}C.

The main complication of the application of the ^{14}C method for groundwater dating arises from the fact that the initial activity A_0, which defines the starting point for the "radioactive decay clock", is possibly affected by geochemical reactions. This is commonly considered using correction models that are either based on the chemical composition of the groundwater, the ^{13}C content of TDIC or both (Eichinger 1983; Fontes and Garnier 1979; Ingerson and Pearson 1964; Mook 1980; Parkhurst et al. 1990). The simplest correction models are basically mixing calculations of different carbon sources in groundwater. The stable ^{13}C is the most suitable mixing parameter because its behaviour is chemically similar to ^{14}C but it undergoes no radioactive decay. Therefore, the concentration of the stable ^{13}C is normalised to the standard carbonate PDB (carbonate from a Pee Dee belemnite) where:

$$\delta^{13}C(PDB) = \left(\frac{{}^{13}C/{}^{12}C_{sample}}{{}^{13}C/{}^{12}C_{standard}} - 1 \right) \cdot 1000\,[‰] \quad (3)$$

Plants that follow the C3 photosynthesis pathway have $\delta^{13}C$ values of ca. –25‰ (Fritz et al. 1985; Mook 1980). CO_2 from root respiration, which has a similar $\delta^{13}C$ value, is dissolved in the water and the resulting carbonic acid drives the dissolution of carbonate minerals in the aquifer. The $\delta^{13}C$ value of marine carbonates is, by definition, equal to zero (Eq. 3). Neglecting isotope exchange reaction (Fontes and Garnier 1979), a $\delta^{13}C$ value of –12.5‰ in TDIC indicates in this pure mixing approach an initial A_0 of 50 pmC. Dating is even more complicated when CO_2 gas from subsurface sources is dissolved in the groundwater. The type of the fermentation reaction determines the isotopic composition of this additional carbon source to the TDIC of the groundwater. For example or CO_2-reduction produces CO_2 enriched in $\delta^{13}C$ (+20‰) and methane (CH_4) which is accordingly depleted in $\delta^{13}C$ (–70‰; Aravena et al. 1995). The ^{14}C activity of CH_4 or CO_2 depends on the age of the decomposed organic matter and the point in time along the groundwater flow when those gases were produced. In the case study reported here, CO_2 from methanogenesis was considered as a third end member in the A_0 mixing calculation.

Sampling and analysis

^{14}C samples were obtained by direct precipitation of TDIC dissolved in several tens of litres of water. For ^{14}C analysis, the precipitated $BaCO_3$ was converted to CO_2 by acidification and CH_4 was synthesised for low level gas counting (Oeschger et al. 1976). The achieved detection limit (DL) is 0.5 pmC. Separate samples (1L) were collected for ^{13}C analysis by mass spectrometry.

Results

^{3}H, ^{3}He, ^{4}He and Ne

The results of the age dating are given in Table 1. Tritium concentrations are below 0.1 TU for samples from depths below 20 mbsl, except for samples from the region Neermoor and the wells in Terborg (Tb3) located closest to the River Ems (Fig. 1). The two shallow Tb3 wells contained tritium concentrations significantly above the tritium concentration in precipitation at the time of recharge (1987). At that time the operation of a nuclear power plant upstream the River Ems started and tritium concentrations in the Ems increased more than one order of magnitude above concentrations in precipitation. For these two samples, the high tritium concentration clearly indicates infiltration from the River Ems.

The tritium concentration in precipitation for the Ems region (IAEA 2006), corrected for decay to year 2006, exceeds 7 TU for the period since 1960. The samples with tritium below 7 TU must contain a tritium-free component, i.e. water infiltrated before 1955. As an example, for well Ro2/14, this tritium-free fraction must be larger than 85%. A natural tritium concentration in precipitation of 4 TU was assumed for this study site, which is 20% lower than for central Germany due to the proximity to the ocean (Roether 1967). The deeper tritium-free samples are therefore older than 80 years, because the residual of 4 TU after 80 years is 0.045 TU. The results of all ^{3}H and ^{3}He analyses and the corresponding ^{3}H–^{3}He-ages are displayed in Fig. 2a.

 DOI 10.1007/s10040-010-0663-4

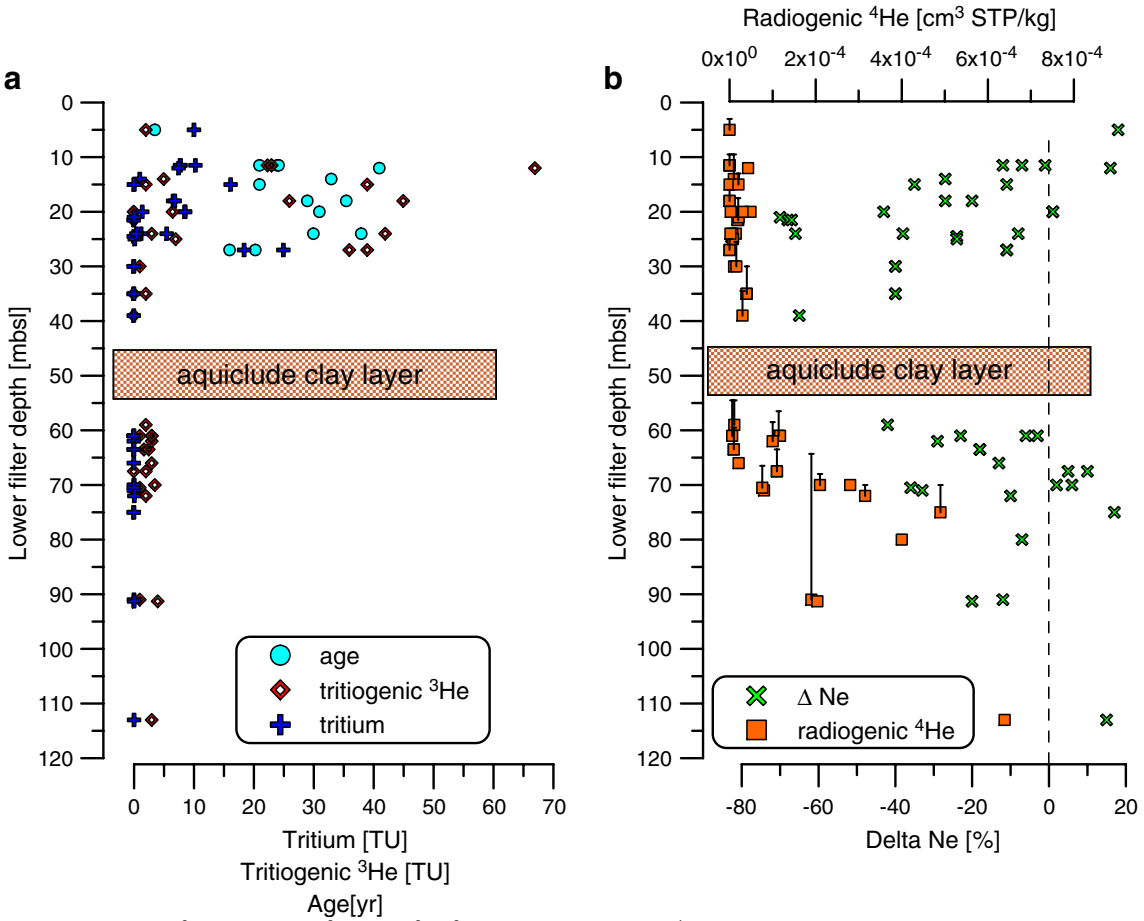

Fig. 2 **a** Concentration of ^{3}H, tritiogenic ^{3}He and ^{3}H–^{3}He age, **b** radiogenic ^{4}He and ΔNe vs. depth. The *vertical bars* at symbols for radiogenic ^{4}He display screen lengths. The approximate position of the clay layer is indicated. The *broken line* indicates ΔNe=0

Ne concentrations are significantly below the solubility equilibrium concentration (ΔNe<0%) except for the shallow samples of Tergast and the deepest samples in the study area (Fig. 2b). The Ne data prove loss of gases from the water body. Maximum degassing ranges between ΔNe –65 to –70% for samples of mid-depths (21–39 m). These samples are free of tritium; therefore, they infiltrated before 1955. Younger waters from shallower wells are affected by degassing also, but not so much. Hence, the gas loss has to be considered in the calculation of tritiogenic ^{3}He and the corresponding ^{3}H–^{3}He ages, and for the accumulation of radiogenic ^{4}He. To do so, there is a need to investigate (1) whether degassing leads to fractionation of gases and (2) the point in time of degassing. It was assumed, that all degassed samples never contained additional atmospheric air, i.e ΔNe was never positive. Consequences of this assumption are specified in Aeschbach-Hertig et al. 2008. To study the first effect, this work focuses on the noble gas isotopes which would be unaffected during aging or affected only marginally, that is (a) ^{4}He for young samples (tritium≥7 TU), (b) ^{3}He for tritium-free samples and (c) Ne.

a and c. Samples with tritium from young water (age <50 yrs) display a small concentration of radiogenic ^{4}He (Fig. 3). Figure 4a shows the ^{4}He and Ne concentration of three sampling periods. Replicate analyses display the same concentration of He and Ne. Degassed samples

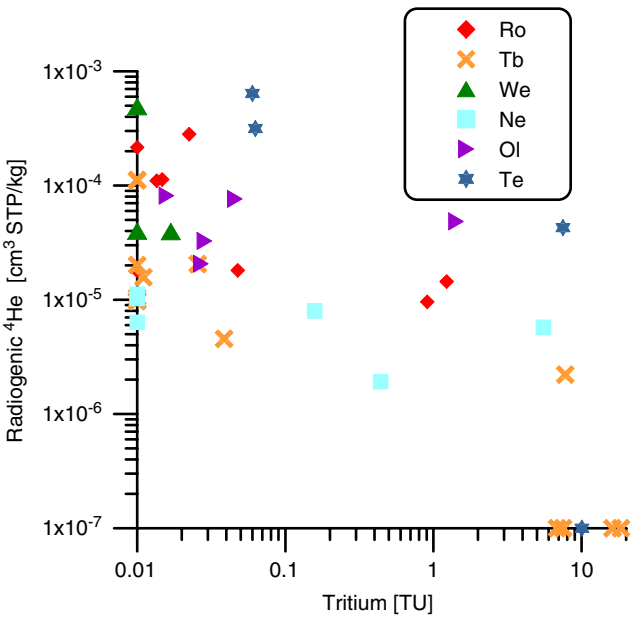

Fig. 3 Radiogenic ^{4}He vs. tritium separated for different areas

DOI 10.1007/s10040-010-0663-4

have Ne concentrations below $2 \cdot 10^{-4}$ cm^3 STP/kg. For degassed samples with low radiogenic ^{4}He, the ^{4}He–Ne relation shows gas loss of equal proportions for He and Ne, indicating no significant fractionation.

b and c. Tritium-free samples could not have produced $^3He_{tri}$ above 10^{-11} cm^3 STP/kg. For tritium-free waters with negligible radiogenic ^{4}He concentration the ^{3}He–Ne relation was used to investigate fractionation (Fig. 4b). Also here, a number of samples showed gas loss of equal proportions and therefore displayed no fractionation during degassing. For comparison a diffusion controlled fractionation (Rayleigh fractionation) for ^{3}He and Ne for degassed water is indicated by the thick blue broken line. All samples fall to the right of this line. For old tritium-free waters a maximum for tritiogenic ^{3}He of 10^{-11} cm^3 STP/kg equivalent to 4 TU (natural tritium in precipitation) is expected. All ^{3}He concentrations are consistent with that upper limit if a small radiogenic component is subtracted (indicated by the black bars at the symbols). According to the long term data records most of old tritium-free non-degassed groundwater samples show tritiogenic ^{3}He significantly below the estimated natural tritium concentration in precipitation. From this one can state: if degassing would have been diffusion controlled, all samples should fall left of the thick blue broken line. As this is not the case it is concluded that degassing reduces the concentrations of the investigated gases (and their isotopes) in equal proportions.

Data of the same well from different sampling periods are generally in very good agreement as are the replicate samples showing the high reliability and quality of sampling and analysis. This was judged as an indicator that degassing did not occur during sampling.

Another substantial issue for ^{3}H–^{3}He dating of degassed samples is the point in time of degassing (Visser et al. 2007). For reasons deduced in the previous and in the following, it was assumed that degassing took place at the time of infiltration. With this assumption, the calculated ^{3}H–^{3}He ages in the depth range of 12–24 mbsl are between 21 and 41 yrs, as already shown in Fig. 2a.

The maximal variation in ^{3}H–^{3}He ages depends on the difference in tritiogenic ^{3}He between the two extreme scenarios (1) degassing during infiltration and (2) degassing during sampling and is represented in Fig. 5. This difference is derived from Eq. 1 where ^{3}He = $^3He_{tri}$:

$$\Delta\tau = \frac{\partial\tau}{\partial^3 He} \cdot \Delta^3 He + \frac{\partial\tau}{\partial^3 H} \cdot \Delta^3 H$$

$$\textit{while tritium is not affected}: \ \Delta^3 H = 0$$

$$\Rightarrow \Delta\tau = \frac{1}{\lambda} \cdot \frac{1}{{}^3He + {}^3H} \cdot \Delta^3 He$$

For tritiogenic ^{3}He for both scenarios from Fig. 5 follows: $\frac{{}^3He(2)}{{}^3He(1)} = \frac{1}{1+\frac{\Delta Ne}{100}}$ and for the difference of tritiogenic ^{3}He:

$$\Delta^3 He = {}^3He(2) - {}^3He(1) = \frac{-\frac{\Delta Ne}{100}}{1+\frac{\Delta Ne}{100}} \cdot {}^3He(1) \quad (\text{note } \Delta Ne < 0)$$

This leads to an estimate for the age difference for the two scenarios depending on the degree of degassing: $\Delta\tau = \frac{1}{\lambda} \cdot \frac{-\frac{\Delta Ne}{100}}{1+\frac{\Delta Ne}{100}} \cdot \frac{{}^3He(1)}{{}^3H + {}^3He(1)}$

For ΔNe=–10% the calculated age would increase by about 2 yrs if ^{3}H << ^{3}He; for ΔNe=–50% the age would increase by 18 yrs.

For samples with tritium below 7 TU, the derived ^{3}H–^{3}He age is not the mean residence time because the age of an old tritium-free component could not be determined. For samples with high concentrations of radiogenic ^{4}He, the separation of tritiogenic ^{3}He is affected by a higher uncertainty, because the ^{3}He/^{4}He ratio of the radiogenic He must be estimated for the aquifer matrix.

The radiogenic ^{4}He is calculated by simply subtracting the atmospheric He portion in the sample from the measured concentration, assuming that the atmospheric He is represented by the atmospheric Ne:

$$\begin{aligned} {}^4He_{rad} &= {}^4He_{sample} - \frac{{}^4He_{equi}}{Ne_{equi}} \cdot Ne_{sample} \\ &= {}^4He_{sample} - (1 + \Delta Ne) \cdot {}^4He_{equi} \end{aligned}$$

Concentrations of $^4He_{rad}$ increased continuously with depth below 60 mbsl, indicating increasing ages with depth. Highest concentrations in the order of $6.4 \cdot 10^{-4}$ cm^3 STP/kg were detected in well Te2/113, which is the deepest (Fig. 2b). Samples with tritium concentration below 7 TU show a significant $^4He_{rad}$ concentration and therefore could be affected by mixing.

^{39}Ar dating

In the depths below 25 mbsl, no ^{39}Ar above the DL was detected (< 10 %modern; Fig. 6). The groundwater residence times in this depth range must, therefore, exceed 900 years. Furthermore the low values indicate that underground production of ^{39}Ar is low in this system. The detectable ^{39}Ar activities observed in the more shallow samples (Table 1), therefore, were directly converted into ages of 130±50 and 250±60 years respectively.

^{14}C dating

Ten samples from the deepest wells have been analysed for the carbon isotopes ^{13}C and ^{14}C of TDIC. The ^{14}C activities of TDIC range between 24 and 68 pmC and the

 DOI 10.1007/s10040-010-0663-4

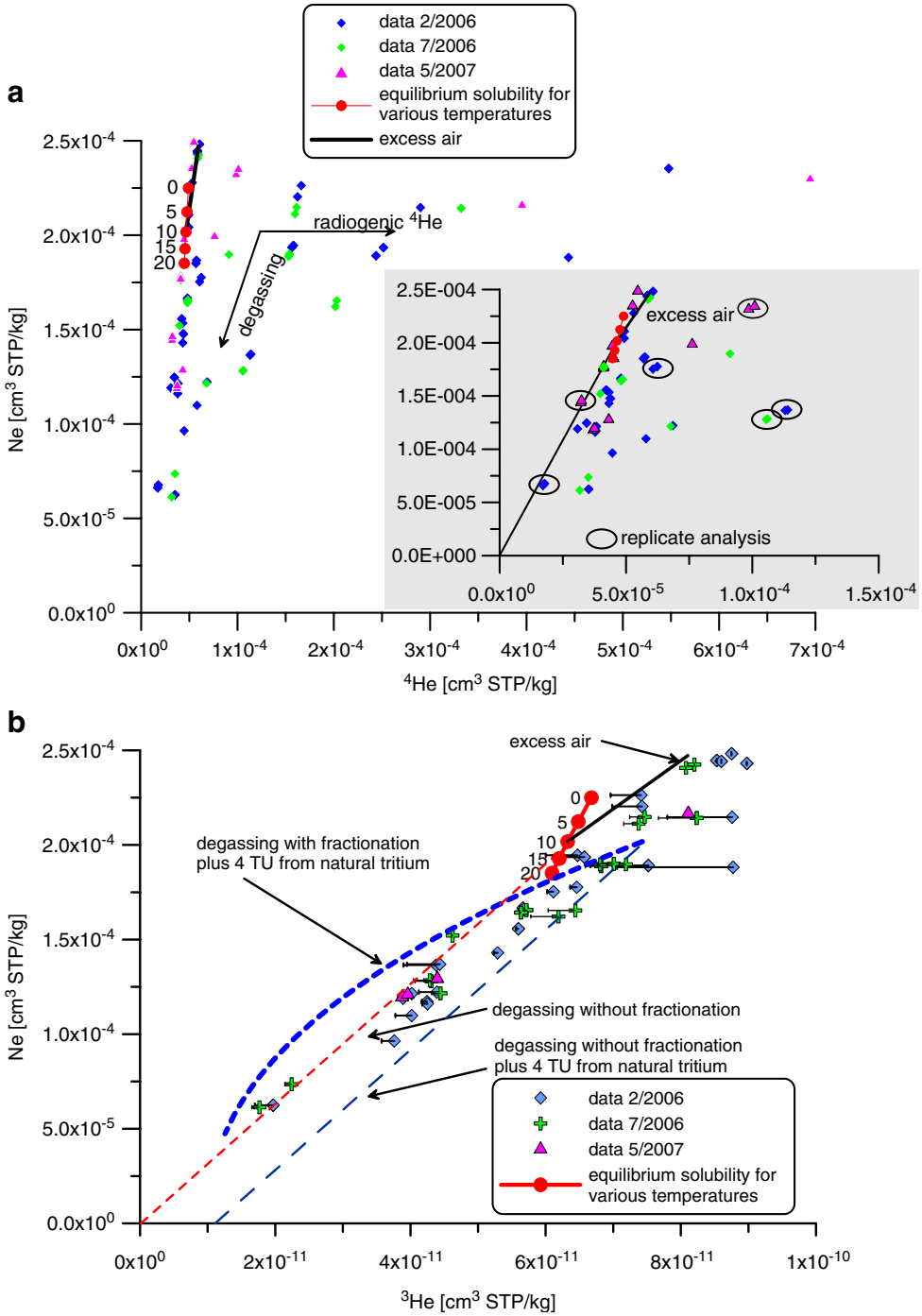

Fig. 4 **a** ^{4}He vs. Ne concentrations for all samples. *Red dots* display solubility equilibrium concentration for fresh water at atmospheric pressure of 1013 hPa for different temperatures. The *excess air line* indicates the extra air with the atmospheric Ne/He ratio dissolved in a sample which is in solubility equilibrium at 10°C. In the enlargement, some replicate measurements are marked. **b** ^{3}He vs. Ne concentrations for samples with tritium <0.1 TU. *Black bars* indicate the amount of radiogenic ^{3}He derived from radiogenic ^{4}He with a radiogenic ^{3}He/^{4}He ratio of $2{\cdot}10^{-8}$. An equivalent of natural tritium in the order of 4 TU=$1{\cdot}10^{-11}$ ^{3}He cm^{3} STP/kg should be found in the samples. If degassing would be controlled by diffusion, data points should fall on or left of the *thick blue broken line*, which was calculated assuming diffusion-controlled degasssing; diffusion constants for He and Ne in water: D_{He}: $5.68{\cdot}10^{-5}$ cm^{2}/s, D_{Ne}: $2.95{\cdot}10^{-5}$ cm^{2}/s at 10°C (Jähne et al. 1987). The diffusion for ^{3}He is derived from ^{4}He by scaling D_{He} with sqrt($mass_{4He}$/$mass_{3He}$)

δ^{13}C values between –21.6 and +1.6 ‰ (Table 1). This large variation in δ^{13}C values is only partly induced by the dissolution of rock carbonates which would cause a much stronger ^{14}C-TDIC reduction than observed (Table 1); Pearson et al. 1991). The investigated waters contained dissolved methane with a δ^{13}C signature of –70±5 ‰ (Table 2), which is typical for bacterially induced methane production (Aravena et al. 1995). Due to isotope fractionation effects that occur during methanogenesis, the simultaneously produced $CO_{2,meth}$ of the reaction becomes

 DOI 10.1007/s10040-010-0663-4

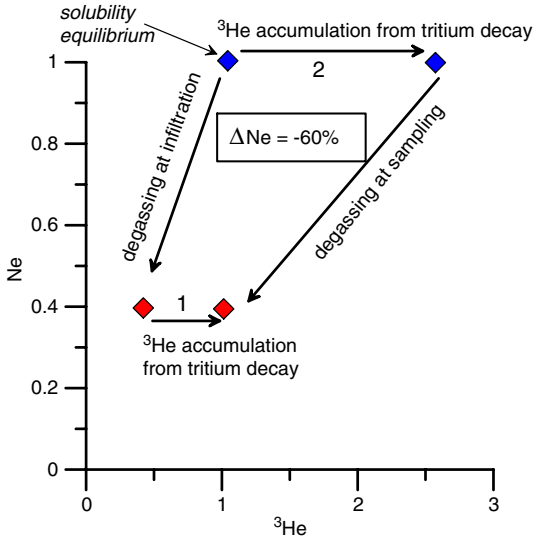

Fig. 5 Two degassing scenarios affecting tritiogenic ^{3}He. *1*: degassing at the time of infiltration, *2*: degassing at sampling

isotopically enriched compared with CH_4 (Balabane et al. 1987, Klass 1984). It is assumed that a $\delta^{13}C$ value of –25 ‰ of decomposed organic matter (Mook 1980) results in a $\delta^{13}C$ of $CO_{2,meth}$ value of +20 ‰ which dissolves in the water and contributes to the TDIC pool (Figs. 7 and 8). Elevated $\delta^{13}C$-TDIC values, therefore, imply a high CH_4 and $CO_{2,meth}$ production. The quasi-linear correlation between $\delta^{13}C$ and ΔNe (Fig. 9) suggest that $CO_{2,meth}$ accumulation is linked to the degassing process. Degassing during sampling is considered to be unlikely as deduced in the previous from the noble gas concentrations. It is, therefore, assumed that degassing occurs by gas stripping in shallow depths during the infiltration process. At a given hydrostatic pressure, $CO_{2,meth}$ is kept much longer in solution than the poorly soluble CH_4. Continuous CH_4 ($+CO_{2,meth}$) production will, therefore, induce the formation of CH_4 bubbles. In the study samples, the highest measured CH_4 concentrations range up to 50 cm^3 STP/L_{water} (Table 2), corresponding to a dissolved gas pressure of about 1.4 atm (solubility of methane: ~35 cm^3 STP/L_{water}/atm). Together with the atmospheric gases remaining in these degassed samples, the total dissolved gas pressure is in the order of 1.5–2 atm, indicating that the depth of methane production is about 5–10 m below groundwater surface. The initially pure methane gas bubbles trigger the ex-solution of atmospheric gases (such as Ne) by gas stripping and the subsequent depletion of those gases in the water phase (Fig. 8 and Brennwald et al. 2005). With increasing methane bubble production the Ne concentration in the water decreases (more negative ΔNe values). The higher $CO_{2,meth}$ input leads to a more enriched $\delta^{13}C$ signature in TDIC (Fig. 8).

Soil organic matter is a complex mixture of substances with an extended range of turnover times generally increasing with depth (Charman et al. 1994; Gillon et al. 2009). As a simplifying hypothesis, three main TDIC sources were identified in the study area's groundwater (Fig. 7).

Source 1. At shallow depths and under aerobic conditions, CO_2 from root respiration ($CO_{2,soil}$) and carbon from relatively fresh organic matter is dissolved in the recharging water. The carbon isotope composition is that of the source plant material, i.e. –25 ‰ and 100 pmC for $\delta^{13}C$ and ^{14}C, respectively.

Source 2. With increasing depth and under anaerobic conditions, $\delta^{13}C$-enriched $CO_{2,meth}$ is increasingly produced as deduced in the previous. The ^{14}C activity of this $CO_{2,meth}$ is related to the age of the fermented bio mass at the location of main methane production. This value is difficult to estimate. It was also observed that ^{14}C ages of dissolved CH_4 and TDIC in peat porewater are much younger than the ^{14}C age of the peat at the same depth (Charman et al. 1994). This reflects the fact that carbon dynamic in peatlands is characterised by a complex mixing pattern. ^{14}C-TDIC of 85 pmC was measured in water of the discharge region of a recent peat bog south of the research area. Similar ^{14}C–CH_4 and ^{14}C-TDIC values were also found in peat bogs elsewhere at a few meters depth (Aravena et al. 1995). A mean ^{14}C activity of 85±10 pmC was consequently assumed for organic matter at depths of maximal methane production. The resultant $CO_{2,meth}$ is ^{14}C-enriched up to 94 pmC due to isotope fractionation. (Because the ^{14}C–^{12}C mass difference is twice that of ^{13}C–^{12}C, the ^{14}C fractionation is approximately twice that of the $\delta^{13}C$: $\Delta^{14}C = 2 \cdot \Delta^{13}C = 2 \cdot 45$ ‰=9 pmC, 85+9=94 pmC)

Source 3. The carbonic acid accumulated in the recharge zone drives the dissolution of carbonate in the aquifer. In the absence of significant subsurface

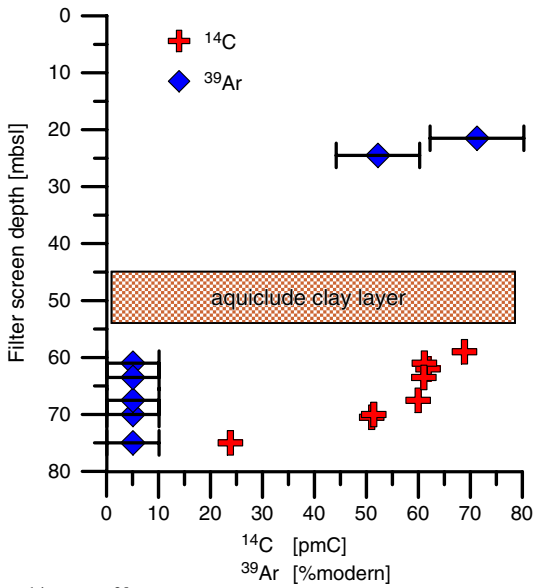

Fig. 6 ^{14}C and ^{39}Ar vs. depth. Below the clay layer the samples are ^{39}Ar free (<10 %modern). For the two shallow wells ^{39}Ar ages of 130 and 250 years were determined

DOI 10.1007/s10040-010-0663-4

Table 2 Concentration, isotope composition and age of methane and TDIC

Sample ID/screen depth (mbsl)	CH_4 (cm^3/L_{water})	$\delta^{13}C_{meth}$ (‰)	$^{14}C_{meth}$ (pmC)	CH_4 age (yrs)	TDIC age[a] (yrs)	TDIC age[b] (yrs)
Gk372/90	0.0	–75.3				
Ro1/22	50.3	–71.2	56.0	2,532		
Ro1/70	8.5	–75.3				
Ro2/61	15.2	–68.2				
Tb2/25	26.4	–73.0				
Tb2/68	11.1	–72.4	64.3	1,386	1,669	1,316
Tb4/64	15.5	–69.7	65.1	1,278	2,031	1,165
PW A71/64	35.3	–68.8	68.6	843	3,407	2,269
Ol1/71	23.7	–73.2	50.5	3,374	3,719	2,650

[a] Calculated with mixing line shown in Fig. 7

[b] Calculated with a constant initial activity of 70 pmC

CO_2 sources, this is the reaction which is commonly considered in ^{14}C correction models (Fontes and Garnier 1979; Mook 1980; Eichinger 1983, Pearson et al. 1991). The ^{14}C dead carbon from the rock matrix (C_{rock}) would dilute the initial carbon isotopic composition towards 0 pmC and $\delta^{13}C$ ~0‰ (Kalin 2000).

The carbon isotope compositions of the three mixing end members (sources 1–3) are depicted in Fig. 7 in a $\delta^{13}C$–^{14}C graph. A ^{14}C-dating-correction procedure requires knowledge of the relative portions (p_1, p_2, p_3) of the three end members for initial ^{14}C activity (A_0) calculation. The remaining activity difference can be attributed to radioactive decay and interpreted in terms of groundwater age. However, because there are three unknowns ($p_{1–3}$) and only two measured parameters ($\delta^{13}C$, ^{14}C), the system of equations is underdetermined. The reference sample Gk372 was used in order to constrain the reaction pathway without methanogenesis. This CH_4-free well is located in the same aquifer but further inland. The absence of ^3H and the ^{39}Ar activity of 80% modern indicate a residence time of 90 years. The low $\delta^{13}C$ value of –21.6‰ indicates a limited availability of carbonate in this aquifer in accordance with the low alkalinities and pH observed. The $\delta^{13}C$–^{14}C mixing line between the reference sample and the assumed $CO_{2,meth}$-endmember (dotted line, Fig. 7) together with the measured $\delta^{13}C$ value defines the initial ^{14}C activity of each sample which is used in the age calculation (vertical arrow in Fig. 7).

The ^{14}C activity of the dissolved methane was measured as a further age constraint. The results from five measured samples range between 50 and 69 pmC. Using again an average initial ^{14}C activity of the decomposed organic matter in the peat bog of 85 pmC, a ^{14}C–CH_4 fractionation factor of $2 \cdot -45$ ‰=–9 pmC (see the previous) and, thus, an initial

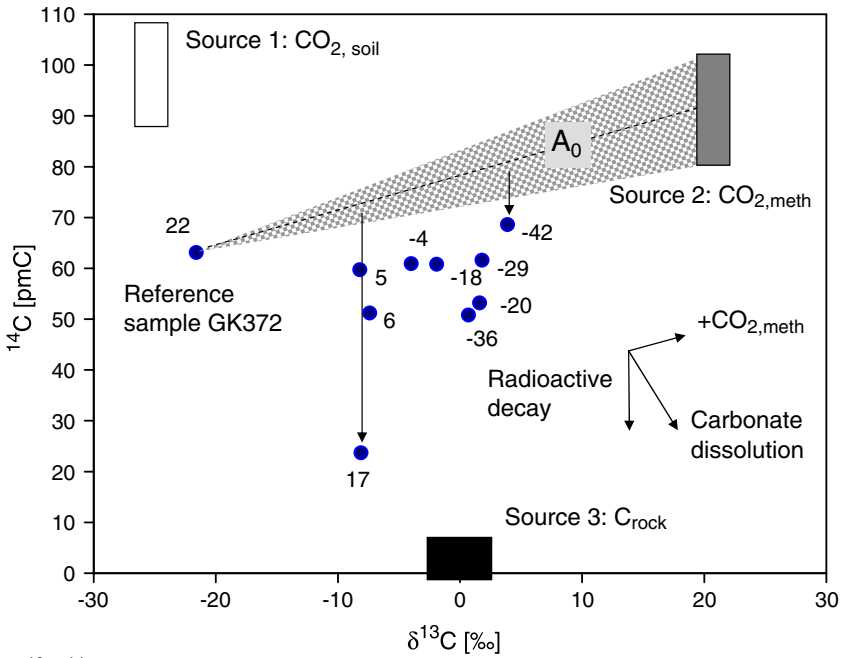

Fig. 7 Carbon isotope ($\delta^{13}C$,^{14}C) composition of groundwater samples and carbon sources for TDIC. The initial ^{14}C activity for radiocarbon dating is estimated based on the mixing between three carbon sources (1–3) with distinct isotopic signatures. The reference sample represents water that is not affected by methanogenesis (no $CO_{2,meth}$; source 2). Labels indicate ΔNe (%) that decrease with increasing $CO_{2,meth}$ (see text and Fig. 9). The *dotted line* corresponds to the initial activity A_o as a function of the $\delta^{13}C$ value of the sample. The lengths of the *vertical arrows* represent aging due to radioactive decay

 DOI 10.1007/s10040-010-0663-4

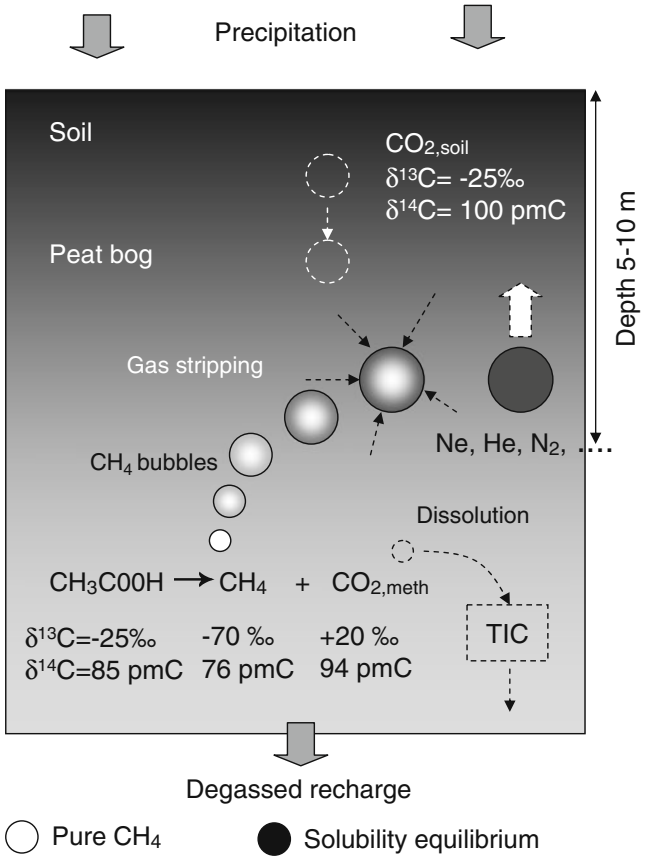

Fig. 8 Scheme of gas stripping in peat bogs. Formation of pure methane bubbles and subsequent gas partitioning of water dissolved gases and gas bubbles. Solubility equilibrium between the water and the gas phase is achieved in steady state. The carbon isotope signature of fermented organic matter, CO_2 and CH_4 are also given. CO_2 stays preferentially in solution due to the 25 times higher solubility compared to methane

CH_4 activity of 76 pmC results in CH_4 ages which are comparable to the ^{14}C-TDIC ages (Table 2). It is thereby assumed that methane behaves conservatively along the flow path (no isotope exchange with the rock matrix or oxidation). The rough correspondence between ^{14}C–CH_4 and ^{14}C-TDIC ages provides additional evidence for the correctness of the basic dating assumptions and the obtained ^{14}C age scale which ranges from 90 yrs for the reference sample up to 9,000 yrs (Table 1).

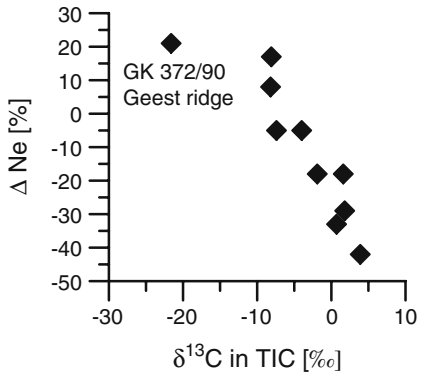

Fig. 9 δ^{13}C in TDIC vs. ΔNe

Discussion

Degassing and dating

Gas stripping or degassing affected the applied dating tracers differently. ^{39}Ar and ^{3}H were not affected at all. ^{14}C, ^{3}He and ^{4}He dating required a careful evaluation of the details of the degassing process. The correlation between δ^{13}C and ΔNe (Fig. 9) suggests that gas stripping is related to methanogenesis, possibly taking place in peat bogs at shallow depths. The continuous production of methane in a low hydrostatic pressure environment induced the formation of initially pure methane bubbles (Fig. 8). The concentration difference of atmospheric gases (Ne, N_2) in air saturated water (ASW) and gas phases (initially pure CH_4) caused the ex-solution of atmospheric gases into the gas bubbles. At the beginning, the degassing process is controlled by the relative diffusion coefficients of the ex-solved gases. The lighter and more mobile gases are enriched in the gas phase during this first non-steady-state phase (Brennwald et al. 2005). In the steady-state equilibrium, however, the partitioning between the water and the gas bubbles is controlled by the relative solubilities of the gases. A detailed discussion of diffusion controlled and solubility controlled degassing processes can be found in Aeschbach-Hertig et al (2008).

Figure 4b shows that ^{3}He and Ne concentrations of the degassed samples were not fractionated. Whereas diffusion-controlled degassing implies a significant fractionation between He and Ne due to the strong difference of diffusion constants, solubility controlled degassing only slightly changes the ratio of He to Ne, as both gases have similar solubilities. The degassing process was probably slow enough to allow solubility equilibrium. Such a slow formation and escape of bubbles was observed in lacustrine sediments (Brennwald et al. 2005) and could also be expected for peat bogs within the research area (Strack et al. 2005). In the beginning of flooding during Holocene transgression phases, the peat bogs grow fast because of banked-up water. After flooding with seawater,

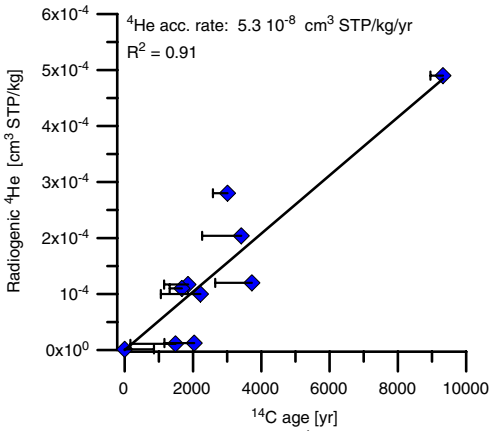

Fig. 10 Concentration of radiogenic ^{4}He concentrations vs. ^{14}C ages calculated according to the mixing scheme in Fig. 7. *Error bars* indicate differences for ^{14}C ages calculated with an initial ^{14}C concentration of 70 pmC

DOI 10.1007/s10040-010-0663-4

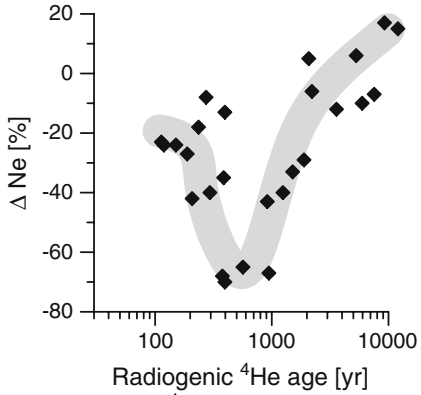

Fig. 11 ΔNe vs. derived ^{4}He ages. *Thick grey line* indicates supposed evolutionary pattern

the peat bogs died and were covered with fine-grained marine sediments (Streiff 1990).

For this study, the application of radiogenic ^{4}He as a dating tool was not affected by degassing, because (1) the water degassed before $^4He_{rad}$ accumulated from the sediments and (2) the atmospheric He component in the sample could be quantified well enough by using the measured Ne concentration of the sample and presuming gas loss of equal portions.

On the much shorter timescales of ^{3}H–^{3}He dating (< 50 yrs), the residence time of the water in the ebullition zone of peat bogs could be significant (years to decades). In principle tritiogenic ^{3}He can escape into CH_4 bubbles during that time interval. Therefore, ^{3}H–^{3}He ages refer to the flow time since the water left the peat bogs. However, at this study site, the highly degassed waters were tritium free and, hence, ^{3}H–^{3}He dating was not applicable anyway.

The initial ^{14}C activity of TDIC and methane for dating of the degassed samples is constrained by the carbon isotopic composition of the fermented organic matter in the peat bog. A three component mixing model between $CO_{2,soil}$ (in the root zone under oxidising conditions), $CO_{2,meth}$ (in a reducing environment) and to a smaller portion carbon from the aquifers' rocks reveal ^{14}C ages which depend on δ^{13}C in TDIC and, thus, on the degree of degassing or CO_2 accumulation respectively. The initial ^{14}C activity in methane (76 pmC) is reduced compared to the ^{14}C activity of the peat bog (85 pmC) due to isotope fractionation during methanogenesis. The resulting $^{14}CH_4$ ages are roughly in agreement with the calculated ^{14}C-TDIC ages (Table 2).

The correlation of ^{14}C ages and $^4He_{rad}$ concentration yield a ^{4}He accumulation rate of $5.3 \cdot 10^{-8}$ $cm^3/kg_{water}/yr$ (Fig. 10). Under the assumption of a similar ^{4}He accumulation rate for all samples $^4He_{rad}$ was used as a regional age proxy. The deduced $^4He_{rad}$ accumulation rate compares well with values found by other researchers: Lehmann et al. (2003): $2–20 \cdot 10^{-8}$ cm^3 STP/kg/yr, Schlosser et al. (1989): $3 \cdot 10^{-7}$ cm^3 STP/kg/yr, Castro et al. (2000): $4 \cdot 10^{-8}$ cm^3 STP/kg/yr and Solomon et al. (1996): $3 \cdot 10^{-7}$ cm^3 STP/kg/yr. A study site with glacial-fluviatile sediments, mainly of a similar structure, 400 km to the east provides nearly the same accumulation rate of $5 \cdot 10^{-8}$ cm^3 STP/kg/yr derived by comparison with ^{14}C ages (Sültenfuß et al. 2006).

Recharge history

Using the constructed ^{4}He ages, the relation of ΔNe vs. age is shown in Fig. 11. Only the oldest (and deepest) waters were unaffected by degassing. In the age range from hundreds to a few thousand years (or the middle depth range 70–30 m), ΔNe values are lowest (most negative) and increase again for the shallower and, thus, younger waters. Water was assigned with ΔNe<0 to be recharged through marshland or peat bogs. The spatial distribution of peat bogs, however, changed over time. The deepest and oldest waters display ΔNe>0 and are supposedly recharged on the Geest ridges. Hence, they were not affected by CH_4 production and likewise gas loss. As these samples are from depths below the degassed samples, they originate from furthest away.

Since about AD 1000, men started building dykes along the River Ems and the North Sea and drained the hinterland. Before that time, the complete area could have

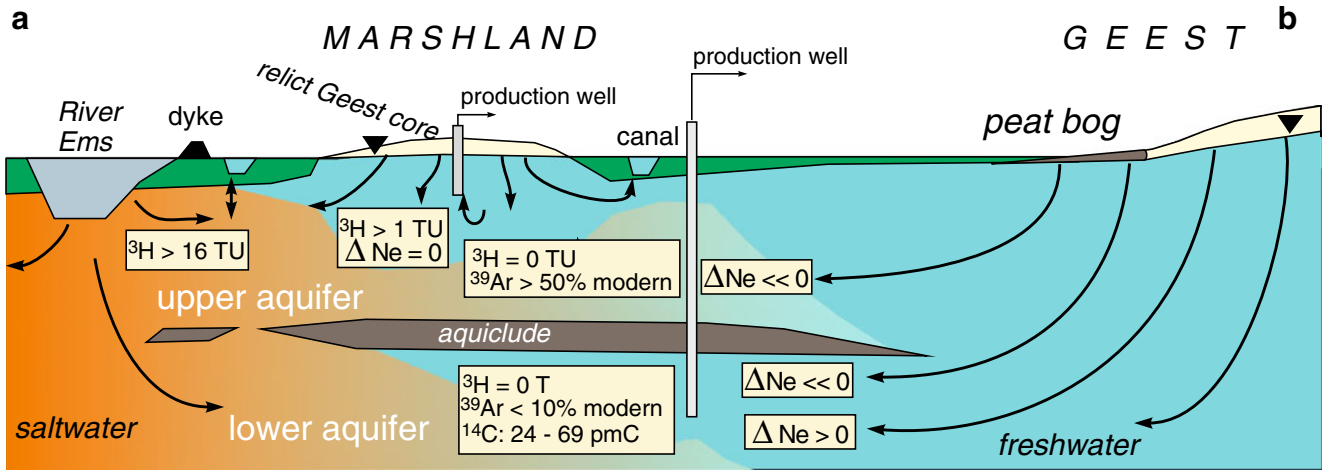

Fig. 12 Schematic of the present-day and past flowpaths within the aquifer along the cross-section **a–b** (Fig. 1). The salt– and freshwater distribution is indicated according to Führböter (2004)

DOI 10.1007/s10040-010-0663-4

acted as a recharge area. After the marshland and peat bogs were drained, the recharge here was interrupted. Since that time groundwater recharged mainly over the Geest ridge and at the Geest humps. Shallow groundwater displays young ^{3}H–^{3}He ages which confirm this concept. The comparison of tritium in wells near the River Ems with water from the River Ems with high tritium produced by a nuclear power plant shows that young brackish water entered the aquifer. At present, young river water intrusion, as indicated by elevated tritium concentrations from the tritium contaminated river Ems, is restricted to few locations close to the river where the river bed is permeable.

From the overall tracer examination, the structure of the aquifer is derived as displayed in Fig. 12. This figure is a composition of recent flowpaths of young waters and ancient flowpaths for the older, deeper water. Due to the sparse and scattered sample spacing, it may be doubtful whether this cross section is applicable for the complete study area. However, the main features of the groundwater dynamics should be well covered.

Conclusions and summary

The groundwater in the investigated section of a coastal aquifer system covers a large range of residence times. In shallow depths below 27 m, most samples contain measurable ^{3}H concentrations and are, therefore, younger than 50 years. ^{3}H–^{3}He ages of the young water components have been determined to 20–41 yrs. Mixing of young water with tritium and tritium-free older water was detected for some samples in shallower depths. Two tritium-free samples in the shallow layer (depths 22–25 m) show groundwater residence times determined by ^{39}Ar measurements of 130 and 250 yrs. This tracer is the best suited tool for groundwater dating on the century time scale. At greater depths, below a low permeability clay layer the ^{39}Ar concentrations drop below 10 %modern, indicating groundwater residence times above 900 years. Additionally, the low ^{39}Ar concentrations in this part of the aquifer demonstrate that underground production is low and does not affect the ^{39}Ar dating. Groundwater ages on the millennium scale were estimated by means of ^{14}C activities in TDIC and methane. A whole set of absolute dating tracers (^{3}H–^{3}He, ^{39}Ar and ^{14}C) provided consistent groundwater ages and allowed an estimate of the ^{4}He accumulation rate. With a nearly constant, ^{4}He release from the aquifer matrix to the water for a finite study site ^{4}He is a sensitive dating tool for a large range of residence times.

Degassing has been observed in most of the samples by means of depleted atmospheric neon concentrations. It was presumed that degassing occurred during groundwater infiltration through peat bogs which covered the area to a large extent before AD 1000. The effect of this gas loss on the applied age dating methods has been discussed. Because degassing occurred at the beginning of the groundwater flow lines and did not fractionate the gases, the separation of $^{3}He_{tri}$ and $^{4}He_{rad}$ was possible and relatively well constrained. ^{39}Ar and ^{3}H concentrations are insensitive to degassing processes.

The temporal and spatial degassing pattern is used as a proxy for groundwater recharge through peat bogs. Groundwater flow and discharge was towards the sea. With the construction of dykes and the drainage of the marshland the water table fell below the level of the River Ems and caused bank filtration of brackish water. This was identified by the high tritium signal from the river.

In this study, the environmental tracers proved their capability as key tools for studying large-scale hydrodynamics. In particular, their combination gave valuable clues for infiltration conditions. For a more detailed study on the degassing processes, the application of the heavier noble gases would be desirable.

Acknowledgements The authors acknowledge the financial support by the Deutsche Forschungsgemeinschaft (DFG, projects: SU 188/1-1 and FU 663/1-1). We would like to thank J. Krull from Stadtwerke Emden GmbH for his support, Prof. Dr. D. Zachmann from TU Braunschweig for sediment analysis and the staff of Oldenburgisch-Ostfriesischer Wasserverband (OOWV) for their technical support. We are thankful to R. Fischer and M. Möll for radiocarbon analyses of TDIC and methane. We thank the Stadtwerke Emden GmbH, Bundesanstalt für Gewässerkunde, Niedersächsischer Landesbetrieb für Wasserwirtschaft, Küstenschutz und Naturschutz (NLWKN) and Wasser- und Schifffahrtsamt Emden for allowing data inspection. The authors also thank Dr. D. Schönwiese from TU Braunschweig and R. Riedmann from University of Bern for assistance in the field. The manuscript was improved thanks to thoughtful comments from K. Walreavens and an anonymous reviewer.

References

Aeschbach-Hertig W, Peeters F, Beyerle U, Kipfer R (1999) Interpretation of dissolved atmospheric noble gases in natural waters. Water Resour Res 35(9):2779–2792

Aeschbach-Hertig W, El-Gamal H, Wieser M, Palcsu L (2008) Modeling excess air and degassing in groundwater by equilibrium partitioning with a gas phase. Water Resour Res 44: W08449. doi:10.1029/2007WR006454

Andrews JN, Lee DJ (1979) Inert gases in groundwater from the Bunter Sandstone of England as indicators of age and palaeoclimatic trends. J Hydrol 41:223–252

Andrews JN, Davis SN, Fabryka-Martin J, Fontes J-C, Lehmann BE, Loosli HH, Michelot J-L, Moser H, Smith B, Wolf M (1989) The in situ production of radioisotopes in rock matrices with particular reference to the Stripa granite. Geochim Cosmochim Acta 53:1803–1815

Aravena R, Wassenaar LI, Plummer LN (1995) Estimating ^{14}C groundwater ages in a methanogenic aquifer. Water Resour Res 31(9):2307–2317

Balabane M, Galimov E, Hermann M, Letolle R (1987) Hydrogen and carbon isotope fractionation during experimental production of bacterial methane. Org Geochem 11:115–119

Benson BB, Krause D (1980) Isotope fractionation of helium during solution: a probe for the liquid state. J Sol Chem 9:895–909

Beyerle U, Aeschbach-Hertig W, Hofer M, Imboden D M, Baur H, Kipfer R (1999) Infiltration of river water to a shallow aquifer investigated with $^{3}H/^{3}He$, noble gases and CFCs. J Hydrol 220:169–185

Brennwald MS, Kipfer R, Imboden DM (2005) Release of gas bubbles from lake sediment traced by noble gas isotopes in the sediment pore water. Earth Planet Sci Lett 235:31–44

Castro MC, Stute M, Schlosser P (2000) Comparison of ^{4}He ages and ^{14}C ages in simple aquifer systems: implications for

groundwater flow and chronologies. Appl Geochem 15:1137–1167
Charman DJ, Aravena R, Barry G, Warner BG (1994) Carbon dynamics in a forested peatland in north-eastern Ontario, Canada. J Ecol 82(1):55–62
Clarke WB, Jenkins WJ, Top Z (1976) Determination of tritium by mass spectrometric measurement of ^{3}He. Int J Appl Radiat Isot 27:515–522
Collon P, Bichler M, Caggiano J, DeWayne C, El Masri Y, Golser R, Jiang CL, Heiz A, Henderson D, Kutschera W, Lehmann BE, Leleux P, Loosli H, Pardo RC, Paul M, Rehm KE, Schlosser P, Scott RH, Smethie WM, Vondrasek R (2004) Developing an AMS method to trace the oceans with ^{39}Ar. Nucl Instrum Methods Phys Res 223–224:428–434
Eichinger L (1983) A contribution to the interpretation of ^{14}C-groundwater ages considering the example of a partially confined sandstone aquifer. Radiocarbon 25:347–356
Fontes J-C, Garnier J-M (1979) Determination of the initial ^{14}C activity of the total dissolved carbon: a review of the existing models and a new approach. Water Resour Res 15(2):399–413
Fritz P, Mozeto AA, Reardon EJ (1985) Practical considerations on carbon isotope studies on soil carbon dioxide. Chem Geol Isot Geosci Sect58(1-2):89–95
Führböter JF (2004) Salz-Süßwasserdynamik im Grundwasser des Ems-Ästuars [Salt- freshwater dynamics in groundwater of the Ems estuary]. Braunschweiger Geowiss. Arb., Bd. 28., BGA, Braunschweig, Germany, 107 pp
Gillon M, Barbecot F, Gibert E, Corcho Alvarado JA, Marlin C, Massault M (2009) Open to closed system transition traced through the TDIC isotopic signature at the aquifer recharge stage, implications for groundwater ^{14}C dating. Geochim Cosmochim Acta 73(21):6488–6501
Hinrichsen D (1998) Coastal waters of the world: trends, threats, and strategies. Island, Washington, DC
IAEA (2006) Isotope hydrology information system. The ISOHIS Database. http://www.iaea.org/water. Cited October 2010
Ingerson E, Pearson FJ Jr (1964) Estimation of age and rate of motion of ground-water by the 14C-method. In: Miyake Y, Koyama T (eds) Recent researches in the fields of hydrosphere, atmosphere and nuclear geochemistry. Maruzen, Tokyo, pp 263–283
Jähne B, Heinz G, Wolfgang D (1987) Measurement of the diffusion coefficients of sparingly soluble gases in water. J Geophys Res 92(C10):10767–10776
Kalin RM (2000) Radiocarbon dating of groundwater systems. In: Cook PJ, Herczeg AL (eds) Environmental tracers in subsurface hydrology. Kluwer, Dordrecht, The Netherlands
Kipfer R, Aeschbach-Hertig W, Peeters F, Stute M (2002) Noble gases in geochemistry and cosmochemistry. In: Porcelli D, Ballentine C, Wieler R (eds) Reviews in mineralogy and geochemistry 47. Mineralogical Society of America, Washington, DC, pp 614–699
Klass DL (1984) Methane from anaerobic fermentation. Science 223:1021–1028
Lehmann BE, Love A, Purtschert R, Collon P, Loosli HH, Kutschera W, Beyerle U, Aeschbach-Hertig W, Kipfer R, Frape SK, Herczeg A, Moran J, Tolstikhin IN, Gröning M (2003) A comparison of groundwater dating with ^{81}Kr, ^{36}Cl and ^{4}He in four wells of the Great Artesian Basin, Australia. Earth Planet Sci Lett 211(3–4):237–250
Loosli HH (1983) A dating method with ^{39}Ar. Earth Planet Sci Lett 63:51–62
Loosli HH, Purtschert R (2005) Rare gases. In: Aggarwal P, Gat JR, Froehlich K (ed) Isotopes in the water cycle: past, present and future of a developing science. IAEA, Vienna, pp 91–95
Lucas LL, Unterweger MP (2000) Comprehensive review and critical evaluation of the half-life of tritium. J Res Nat Inst Stand Technol 105:541–549
Mamyrin BA, Tolstikhin IN (1984) Helium isotopes in nature. Elsevier, Amsterdam
Massmann G, Sültenfuß J, Dünnbier U, Knappe A, Taute T, Pekdeger A (2008) Investigation of groundwater residence times during bank filtration in Berlin: a multi-tracer approach. Hydrol Proced 22:788–801
Massmann G, Sültenfuß J, Pekdeger A (2009) Analysis of long-term dispersion in a river-recharged aquifer using tritium/helium data. Water Resour Res 45:W02431. doi:10.1029/2007WR006746
Mook WG (1980) Carbon-14 in hydrogeological studies. In: Fritz P, Fontes JCH (eds) Handbook of environmental isotope geochemistry, vol 1. Elsevier, Amsterdam, pp 49–74
Oeschger H, Lehmann B, Loosli HH, Moell M, Neftel A, Schotterer U, Zumbrunn R (1976) Recent progress in low level counting and other isotope detection methods. 9th International Radiocarbon Conference, University of California Press, Berkeley, CA
Parkhurst DL, Thorstenson DC, Plummer LN (1990) PHREEQE: a computer program for geochemical calculations. US Geol Surv Water Resour Invest Rep 80-96, 195 pp
Pearson FJ Jr, Balderer W, Loosli HH, Lehmann BE, Matter A, Peters T, Schmassmann H, Gautschi A (1991) Applied isotope hydrogeology: a case study in northern Switzerland. In: Studies in environmental science, 43, Elsevier, Amsterdam
Purtschert R, Love A, Beyerle U (2007) Constraining groundwater residence times in a fractured aquifer using noble gas isotopes. Goldschmidt Conf. Abstracts 2007, A813, Goldschmidt 2007, Cologne, Germany
Roether W (1967) Estimating the tritium input to groundwater from wine samples: groundwater and direct run-off contribution to central European surface waters. In: Isotopes in hydrology, IAEA, Vienna, pp 73–91
Schlosser P, Stute M, Dörr H, Sonntag C, Münnich KO (1988) Tritium/^{3}He dating of shallow groundwater. Earth Planet Sci Lett 89:353–362
Schlosser P, Stute M, Sonntag C, Münnich KO (1989) Tritiogenic ^{3}He in shallow groundwater. Earth Planet Sci Lett 94:245–254
Solomon DK (2000) ^{4}He in groundwater. In: Cook PJ, Herczeg AL (eds) Environmental tracers in subsurface hydrology. Kluwer, Dordrecht, The Netherlands
Solomon DK, Cook PC (2000) ^{3}H and ^{3}He. In: Cook PJ, Herczeg AL (eds) Environmental tracers in subsurface hydrology. Kluwer, Dordrecht, The Netherlands
Solomon DK, Schiff SL, Poreda RL, Clarke WB (1993) Validation of the ^{3}H/^{3}He method for determining groundwater recharge. Water Resour Res 29(9):2951–2962
Solomon DK, Hunt A, Poreda RJ (1996) Source of radiogenic helium-4 in shallow aquifers: implications for dating young groundwater. Water Resour Res 32(6):1805–1813
Stadtwerke Emden GmbH (2006) Beweissicherungmaßnahmen für Grundwasserentnahme im Wasserwerk Tergast (Fassungsanlagen Tergast und Simonswolde) - Hydrogeologischer Jahresbericht 2005 [Annual hydrogeological report 2005 for waterwork Tergast, catchment Tergast and Simonswolde]. Stadtwerke Emden, Emden Stadt, Germany
Strack M, Kellner E, Waddington JM (2005) Dynamics of biogenic gas bubbles in peat and their effects on peatland biogeochemistry. Glob Biogeochem Cycles 19:GB1003. doi:10.1029/2004GB002330
Streiff H (1990) Das ostfriesische küstengebiet [The eastern Frisian coastal area]. Sammlung geologischer Führer, Bd. 57, Borntraeger, Berlin
Stute M, Deák J, Révész K, Böhlke JK, Deseö É, Weppernig R, Schlosser P (1997) Tritium/^{3}He dating of river infiltration: an example from the Danube in the Szigetköz area, Hungary. Ground Water 35(5):905–911
Stuyfzand PJ (1996) Salinization of drinking water in the Netherlands: anamnesis, diagnosis and remediation. 14th Saltwater Intrusion Meeting Proceedings, Malmö, Sweden, pp 168–177
Sültenfuß J, Weise SM, Osenbrück K, Bednorz F, Brose D, Robert C (2006) Radiogenes ^{4}He als Alterstracer für Grundwasser [Radiogenic ^{4}He as age tracer for groundwater]. Verhandlungen der Deutschen Physikalischen Gesellschaft 2006, Heidelberg, Germany. http://www.dpg-verhandlungen.de/2006/heidelberg/up2.pdf. 1 September 2009
Sültenfuss J, Rhein M, Roether W (2009) The Bremen mass spectrometric facility for the measurement of helium isotopes, neon, and tritium in water. Isot Environ Health Stud 45(2):1–13

Szabo Z, Rice DE, Plummer LN, Busenberg E, Drenkard S, Schlosser P (1996) Age dating of shallow groundwater with chlorofluorocarbons, tritium/ helium-3 and flow path analysis, southern New Jersey coastal plain. Water Resour Res 32:1023–1038

Tolstikhin IN, Kamenskiy IL (1969) Determination of groundwater ages by the ^{3}H–^{3}He method. Geochem Int 6:810–811

Torgersen T, Clarke WB (1985) Helium accumulation in groundwater: an evaluation of sources and the continental flux of crustal ^{4}He in the Great Artesian Basin, Australia. Geochim Cosmochim Acta 49:1211–1218

Torgersen T, Clarke WB, Jenkins WJ (1979) The tritium/helium-3 method in hydrology. Isotope Hydrology 1978, IAEA Symposium 228, Neuherberg, Germany, June 1978

Visser A, Broers HP, Bierkens MFP (2007) Dating degassed groundwater with $^{3}H/^{3}He$. Water Resour Res 43:W10434. doi:10.1029/2006WR005847

Weiss RF (1971) Solubility of helium and neon in water and seawater. J Chem Eng Data 16:235–241

Weise SM, Moser H (1987) Groundwater dating with helium isotopes. In: Isotope techniques in water resources development, IAEA, Vienna, pp 105–126